Computers and Concrete, *Vol. 25, No. 2 (2020) 145-154*
DOI: https://doi.org/10.12989/cac.2020.25.2.145

Study on the propagation mechanism of stress wave in underground mining

Fei Liu*[1] and Lianghui Li[2]

[1]Guangdong Provincial Key Laboratory of Deep Earth Sciences and Geothermal Energy Exploitation and Utilization, Institute of Deep Earth Sciences and Green Energy, College of Civil and Transportation Engineering, Shenzhen University, Shenzhen, 518060, China
[2]College of Energy & Mining, China University of Mining & Technology, Beijing 100083, China

(*Received November 18, 2019, Revised January 30, 2020, Accepted February 4, 2020*)

Abstract. For the influence of the propagation law of stress wave at the coal-rock interface during the pre-blasting of the top coal in top coal mining, the ANSYS-LS/DYNA fluid-solid coupling algorithm was used to numerical calculation and the life-death element method was used to simulate the propagation of explosion cracks. The equation of the crushing zone and the fracturing zone were derived. The results were calculated and showed that the crushing radius is 14.6 cm and the fracturing radius is 35.8 cm. With the increase of the angles between the borehole and the coal-rock interface, the vibration velocity of the coal particles and the rock particles at the interface decreases gradually, and the transmission coefficient of the stress wave from the coal mass into the rock mass decreases gradually. When the angle between the borehole and the coal-rock interface is 0°, the overall crushing degree is about 11% and up to the largest. With the increase of the distance from the charge to the coal-rock interface, the stress wave transmission coefficient and the crushing degree of the coal-rock are gradually decreased. At the distance of 50 cm, the crushing degree of the coal-rock reached the maximum of approximately 12.3%.

Keywords: coal-rock interface; stress wave; crushing degree; transmission coefficient

1. Introduction

Top coal mining is usually used for mining underground thick coal seams, which is due to the superiority of safe and efficient mining in fully mechanized top coal caving (Wang *et al*. 2017, Yasitli and Unver 2005, Li 2018, Li 2017, Xu 2019). However, it cannot be used in the steeply inclined thick coal seams for the hard and the clamping effect of the top coal and the short working face. Most of the coal mines in western of China are steeply inclined ultra-thick coal seams. For example, the structure of steeply inclined coal seams in Wudong mine are shown as follows (Wang 2017).

As shown in Fig. 1, the slicing top-coal caving mining was used in steeply inclined thick coal seams by Shenhua Xinjiang Energy Co. Ltd. in Wudong mine. At present surface mining has reached the +500 m level (+850 m on) (Fig. 1). The technology of top coal weakening blasting is

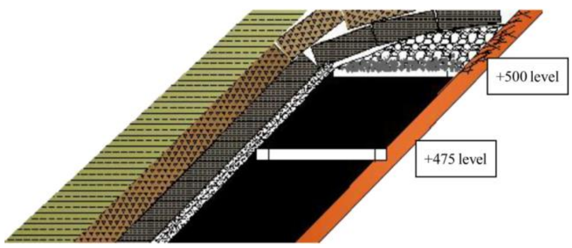

Fig. 1 Panel layout for slicing top-coal caving mining in Wudong mine (Wang 2017)

*Corresponding author, Ph.D.
E-mail: feiliu182@163.com

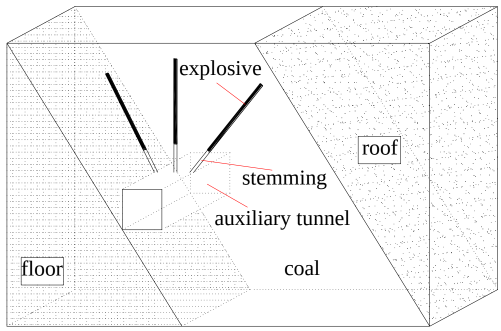

Fig. 2 Horizontal section top coal caving

an effective way for the top coal can hardly broke at that inclination and thickness (Cai-ping *et al*. 2012, Bossart *et al*. 2002). That is, the auxiliary tunnel is arranged in the top coal to implement the weakening and crushing control technology for the top coal, so that the top coal can be smoothly discharged, and then the top coal mining technology can be used successfully (Wang *et al*. 2013, Li *et al*. 2009).

The coal seam in Jiangcang mine also has a large dip more than 45º. As researched on the 45# coal seam in this paper, the Horizontal Section Top Coal Caving (HSTCC) method was used as shown in Fig. 2.

As shown in Fig. 2, the coal seam was divided into two horizontal sections. Two auxiliary tunnels were implemented in different heights and the boreholes were drilled in the coal from the auxiliary tunnel. The top coal was broken for a smoothly caving after the explosives detonating. However, to study on the influence of the interface between the coal and the roof on propagation of the explosion-induced stress wave, different angles between

ISSN: 1598-8198 (Print), 1598-818X (Online)

the interface and the boreholes were set up in this paper.

The top coal pre-blasting technology in fully mechanized caving mining in hard and thick seam is systematically studied through laboratory blasting test, fractal theory analysis, 3D FLAC numerical calculation and related engineering comparison by Wang *et al.* (2000). And the reasonable pre-blasting scheme and parameters are proposed, and the distribution of top coal briquettes before and after pre-blasting was analyzed by using the topology theory. Yang (2015) developed a new technology of pressure blasting for the conditions of hard and thick sandstone roof in coal mines, and implemented the directional control blasting under roof pressure-bearing on the working face and the side of the mining roadway respectively. So as to realize the two-way unloading of the surrounding rock of the stope and the transfer of high stress to ensure the production of the working face safely and efficiently. Suo (2004) proposed the calculation method of the hard top coal weakening blasting area, fracture development area and fissure area, and shown the function of fragmentation degree of the top coal by adopting the pre-blasting weakening technology and experiments and field observations.

The research on the propagation of explosive stress waves and the fractures of coal and rock at the interface is important (Fei *et al*. 2019, Saiang 2009, Yan *et al*. 2015, Pradhan *et al*. 2018, Adibi *et al*. 2019). This paper uses ANSYS/LS-DYNA numerical calculation method to simulate the propagation of explosive stress wave at the interface of top coal and roof on the basis of summarizing the previous studies. The angle and the distance between the borehole and the coal-rock interface are set up differently to study the fracture effect of the explosion stress wave on the coal and rock.

2. Detonation mechanisms

The detonation velocity of a cylindrical charge is greatly affected by the diameter of the explosive. Within a certain range, the detonation velocity increases with the increase of the diameter until the steady detonation velocity is reached; and as the diameter decreases, the detonation velocity decreases until the critical diameter is reached and the detonation cannot be transmitted and fails (Cooper 1996). This is mainly due to the fact that the detonation process of the column charge is affected by the lateral pressure of the charge. The non-ideal detonation state, as shown in Fig. 3 below, the front of the shock wave propagates in a curved shape followed by a chemical reaction zone that is not completely reacted. The chemical reaction zone is followed by a jet-like propagating product (Esen 2008).

As shown in Fig. 3, the detonation drive zone (DDZ) is located at the front of the sonic line and follows with the shock wave front, and drives the detonation process to propagate in the explosive (Byers 2002). At this time, the detonation speed is close but still less than the ideal detonation speed. The non-ideality degree of explosives can be judged by the difference between the ideal detonation speed and the actual detonation speed. The sparse wave (also known as Taylor wave) located between the sonic line and the end of the reaction zone is still supersonic. Therefore, the disturbances of compression waves and sparse waves that propagate at the local sound velocity are still lag behind the DDZ, so the propagation speed of the detonation wave cannot be slowed down. Taylor waves are still having chemically reactive, and for industrial explosives with slower energy release rates, Taylor waves are critical to the explosion process (Byers 2002).

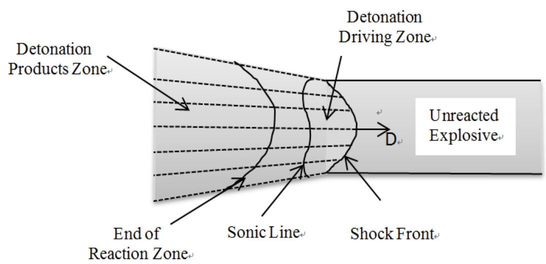

Fig. 3 Non-ideal detonation representation

For the blasting of the cylindrical charge in the coal, the boreholes at both ends of the charge are subjected to a strongly effect of impact compression by the explosive stress wave and the jet-liked detonation product along with the radial direction of the borehole (Nicieza *et al*. 2012). The coal surrounding the lateral of charge is subjected to the effect of the explosion stress wave that expands outward in a cylindrical shape.

3. Blasting damage zone

3.1 Crushing zone

In this paper, the charge and the borehole are treated as coupled. When the coupled columnar charge is detonated, the initial pressure of the shock wave in the coal can be treated according to the acoustic approximation principle (Yang 1993, Zhang 1998) as follow.

$$P_r = \frac{2\rho C_p}{\rho C_p + \rho_m C_v} P_m \tag{1}$$

In this equation, ρ and ρ_m is the density of coal and explosive, respectively, in Kg·m^{-3}. C_p and C_v is the sonic velocity in coal and detonation velocity of explosives, respectively, in m·s^{-1}. P_m is the detonation pressure of the explosives, in Pa.

According to the detonation mechanics, the detonation pressure of the explosives (P_m) can be shown as follow.

$$P_m = \frac{1}{4}\rho_m C_v^2 \tag{2}$$

So, the initial pressure of the shock wave in the coal can be shown according to the Eq. (1) and Eq. (2) as follow.

$$P_r = \frac{\rho\rho_m C_p C_v^2}{2(\rho C_p + \rho_m C_v)} \tag{3}$$

The energy of the explosion shock wave decays rapidly during the process of the propagation. The relationship between the variations of the peak pressure of the shock wave near the borehole and the distance from the borehole can be shown as follow.

$$p(\bar{r}) = \frac{p_r}{\bar{r}^{\alpha_1}} \tag{4}$$

In the equation, $\bar{r}$ is the proportional distance which can be shown as $\bar{r} = r/r_b$. r is the distance from the center of the explosive, in m. r_b is the radius of the borehole. α_1 is the attenuation index of the shock wave pressure, which can be shown as follow.

$$\alpha_1 = 2 + \frac{\mu_d}{1-\mu_d} \tag{5}$$

In the equation, μ_d is the dynamic Poisson's ratio of coal. As in the coal blasting engineering, the μ_d is always be equal to 0.8μ. μ is the static Poisson's ratio.

Dai (2002) researched the criterion for the range of the coal blasting crushing area according to the Mises yield failure criterion as follow.

$$\sigma_i \geq \sigma_{cd} \tag{6}$$

In this equation, σ_{cd} is the dynamic compressive strength of the coal, in MPa. σ_i is the stress at any point in the coal which can be shown as follow.

$$\sigma_i = \frac{1}{\sqrt{2}}[(\sigma_r - \sigma_\theta)^2 + (\sigma_\theta - \sigma_z)^2 + (\sigma_z - \sigma_r)^2]^{1/2} \tag{7}$$

In the equation, σ_r is the radial stress of the point in the coal, in MPa. σ_θ is the tangential stress, in MPa. σ_z is the stress in the direction of the borehole, in MPa.

As the explosion wave propagating in the coal, the shock wave is gradually attenuated into a stress wave for the hindered of the coal. The stress field in the coal is regarded as a plane strain problem. At this time, the three-dimensional stress in the coal is shown as follow.

$$\begin{cases} \sigma_r = p_{R_c}/\bar{r}_c^{\,\alpha_2} \\ \sigma_\theta = -b\sigma_r \\ \sigma_z = \mu_d(1-b)\sigma_r \end{cases} \tag{8}$$

In the equation, p_{R_c} is the peak stress at the interface (R_c) between the crushing zone and the fracturing zone. The proportional distance $\bar{r}_c$ can be shown as $\bar{r}_c = r/R_c$. α_2 is the peak stress decay index, which can be expressed as $\alpha_2 = 2 - \mu_d/(1-\mu_d)$ (Ханукаев 1980). b is the lateral stress coefficient, which can be shown as $b = \mu/(1-\mu)$.

The radial stress σ_r can be shown by relating the Eq. (8) as follow.

$$\sigma_i = \frac{1}{\sqrt{2}}\sigma_r[(1+b)^2 - 2\mu_d(1-\mu_d)(1-b)^2 + 1 + b^2]^{1/2} \tag{9}$$

According to the Eqs. (3)-(4), Eq. (6) and Eq. (9), the radius of the crushing zone in the coal by using coupled charge can be shown as follow.

$$R_c = \left(\frac{\rho_m C_v^2 AB}{4\sqrt{2}\sigma_{cd}}\right)^{1/\alpha_1} r_b \tag{10}$$

In the equation

$$A = \frac{2\rho C_p}{\rho C_p + \rho_m C_v} \tag{11}$$

$$B = [(1+b)^2 - 2\mu_d(1-\mu_d)(1-b)^2 + 1 + b^2]^{\frac{1}{2}} \tag{12}$$

3.2 Fracturing zone

According to the Mises yield failure criterion, the

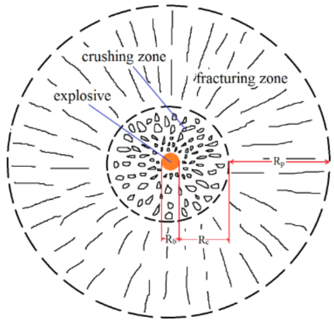

Fig. 4 Damage zone

criterion for the range of the coal fracturing zone was given by Dai (2002) as follow.

$$\sigma_i \geq \sigma_{td} \tag{13}$$

In the equation, σ_{td} is the dynamic tensile strength of the coal.

The fracturing zone is where the tensile stress in the coal is greater than the tensile strength of the coal. According to the Eq. (9), Eqs. (12)-(13), the radial stress (σ_R) on the interface between the crushing zone and the fracturing zone can be shown as follow.

$$\sigma_R = \sigma_{r|r=R_c} = \frac{\sqrt{2}\sigma_{td}}{B} \tag{14}$$

According to the Eq. (8), Eq. (10) and Eq. (14), the radius of the blasting fracturing zone in the coal under coupled charging can be shown as follow.

$$R_p = \left(\frac{\sigma_{cd}}{\sigma_{td}}\right)^{1/\alpha_2} \left(\frac{\rho_m C_v^2 AB}{4\sqrt{2}\sigma_{cd}}\right)^{1/\alpha_1} r_b \tag{15}$$

3.3 Calculation results of the damage zone

The damage zone in the coal after blasting can be shown as Fig. 4. Due to the vibrating zone do not create fractures in the coal, it was not considered in this paper.

The Emulsion was used as the explosive in this paper and the papermeters was given as follows. The density of the explosive ρ_m is 890 $Kg{\cdot}m^{-3}$, and the detonation velocity of the explosive C_v is 4688 $m{\cdot}s^{-1}$. The parameters for the coal material in this paper were citated from the Wudong mine (Hao 2016) as follows. The density of the coal ρ is 1860 $Kg{\cdot}m^{-3}$; the sonic velocity in the coal C_p is 650 $m{\cdot}s^{-1}$; Poisson's ratio is 0.3; the dynamic compressive strength is 69.67 MPa and the dynamic tensile strength is 15.6 MPa.

By using the parameters above, the radius of the crushing zone and fracturing zone in the coal under coupled charging can be calculated. According to the Eq. (10) and Eq. (15), the crushing radius and fracturing radius can be calculated as $R_c = 0.146$ m and $R_p = 0.358$ m, respectively.

4. Calculation model

4.1 Modeling

The model shown in Fig. 5 is established as follows.

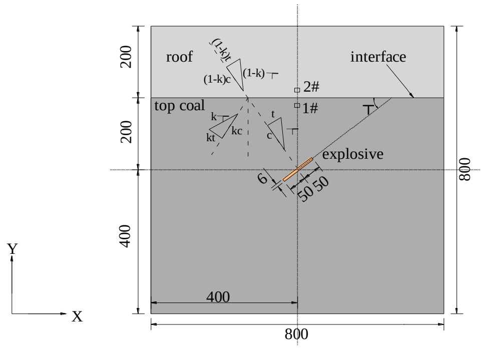

Fig. 5 Design diagram of model (unit cm)

The size of the model is 800×800×2 cm. The roof is made up of rock with a horizontal interface between the top coal and the roof. The coordinate axis is shown on the left, where the *Z*-axis direction is outwardly perpendicular to the paper surface, and the specific dimensions are shown in Fig. 5.

The explosive is detonated by using a reverse point detonation method, the terminal effect is ignored, and the model is simplified to be a plane strain problem. In order to reduce the calculation, a single-layer solid mesh modeling is adopted, and the unit system cm-g-μs is adopted. The length of the charge is 100 cm and the diameter is 6 cm, the charge center is coincides with the model center. The measuring points 1#, 2# are located in the coal and the rock near the interface of the coal and rock respectively, and located on the vertical axis of the model. The charge axis and the coal and rock interface are at an angle of θ. The charging center is fixed, and the angle between the charge and the coal and rock interface is 0°, 30°, 45°, 60° and 90°, respectively.

The propagation of the explosion stress wave at the interface of coal and rock is studied by setting the angle between the charge axis and the interface of the coal and rock. As shown in Fig. 5, the stress wave generated by the explosion changes when it encounters the interface of the coal and rock. It forms an incident wave entering the rock and a reflected wave reflected back to the coal. The incident wave causes compression damage to the rock, and the reflected wave forms tensile damage to the coal.

The numerical model consists of explosive, coal and rock. ANSYS/LS-DYNA finite element software is used to analyze the nonlinear dynamic response of the structure. The explosive is defined as fluids and modeled by Euler meshes, and the units using the multi-substance ALE algorithm. The coal and rock are defined as Lagrange units, and the ALE fluid-solid coupling algorithm is used to establish the connection between them. So the explosive unit can flow into the grid to avoid serious distortion of the unit (Shi *et al*. 2005, Liu and Bai 2019, Prabhat *et al*. 2019, Reza and Kiachehr 2019). The established model is meshed by sweep meshing, and the model meshing result is shown as follows in Fig. 6 as θ is 45°.

The model boundary is set as NON_REFLECTED_BOUNDAY to simulate an infinite boundary condition. The invalid keyword *MAT_ADD_EROSION (LSTC 2003) is set to define that

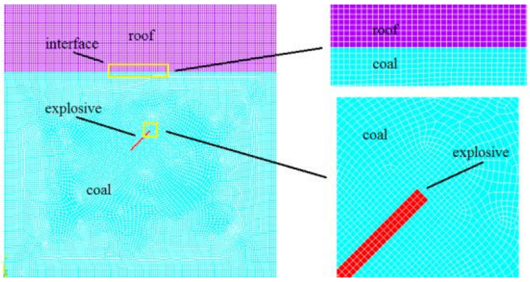

Fig. 6 Meshing diagram

when the coal and rock unit are under excessive force, the overstressed element is automatically deleted. The cracks are formed macroscopically, and the expansion law of the explosion cracks in the coal and the final crushing results of coal and rock are analyzed (Bai 2005).

4.2 Constitutive equation and material parameters

The detonation velocity and pressure of various explosives and the metal accelerated experiments were done by Kury *et al*. (1965), Lee *et al*. (1968). The adiabatic expansion equation of detonation products is described by pressure, volume and energy (PVE). The Jones-Wilkens-Lee (JWL) equation of state based on the thermodynamics and fluid mechanics was given by relating the pressure and specific volume generated in the detonation process which had been widely used in blasting calculations. It can be used as follows.

$$P = A\left(1-\frac{\omega}{R_1 V}\right)e^{-R_1 V} + B\left(1-\frac{\omega}{R_2 V}\right)e^{-R_2 V} + \frac{\omega E_0}{V} \quad (16)$$

In the Eq. (16), A and B are characteristic parameters of the material, in GPa. R_1, R_2, and ω are also parameters of the material. P is pressure, in MPa. V is the relative volume, in m3, and $E0$ is the initial specific internal energy, in MJ.

Jose *et al.* (2015) tested a variety of emulsions and ANFO explosives by using the method of copper column expansion measurements and obtained the specific JWL state parameters of the explosives. The Titan-6000-E1 emulsion was used as the high-energy explosive material in this paper for the numerical simulation. The parameters and the JWL of the explosive are shown in the following tables.

The constitutive of the material will be changed greatly under the explosion dynamic loading. By following the procedures of the LS-DYNA keyword user's manual, the material properties of coal were implemented in the model (Shang *et al*. 2005).

The constitutive behavior selected for coal was of type Plastic-Kinematic, which is suited to model kinematic hardening plasticity with the option of including strain-rate effects. The parameters for the coal and rock material are included in Table 3.

5. Results and analysis

5.1 Different angles

The material parameters and the equation of state are

Table 1 Material parameters of Titan-6000-E1 emulsion

Density/ρ_0 (Kg·m^{-3})	Detonation velocity /D (m·s^{-1})	CJ Pressure/ P_{CJ} (GPa)	CJ Relative volume/ V_{CJ}	Ideal explosion heat/ Q (KJ/Kg)
890	4688	374	7.33	4.15

Table 2 JWL state parameters of Titan-6000-E1 emulsion

A (GPa)	B (GPa)	C (GPa)	R^1	R^2	ω	E_0 (GPa)
209.685	3.509	0.517	5.762	1.290	0.39	2.386

Table 3 Material parameters of coal

Material Type	Density/ρ_0 (Kg·m^{-3})	Elastic modulus /E (MPa)	Poisson's ratio	Yield stress (KN)	Tangent modulus (MPa)	Hardening coefficient	Failure strain
Coal	1860	2610	0.3	1.0	2.61	0.5	0.8
Rock	2650	40000	0.2	100	4000	0.5	0.6

applied into the LS-DYNA with the damage model. The established model was numerically calculated and the explosive was detonated by the point detonation method. The calculation results are post-processed and analyzed, the explosive unit is hidden, and the blast wave propagation and crack propagation process are intercepted as shown in Fig. 7.

Fig. 7 shows the crushing process of the coal when the angle between the charge and the coal and rock interface is different. Among them, the explosion process at different moments are the stress wave reaches the interface of coal and rock, the tensile cracks formed and the final fracture of the coal and rock, respectively. It can be seen from the figure that the propagation velocity changes when the stress wave reaches the interface of the coal and rock. The propagation velocity of the stress wave is obviously accelerated when it enters the rock from the coal. A

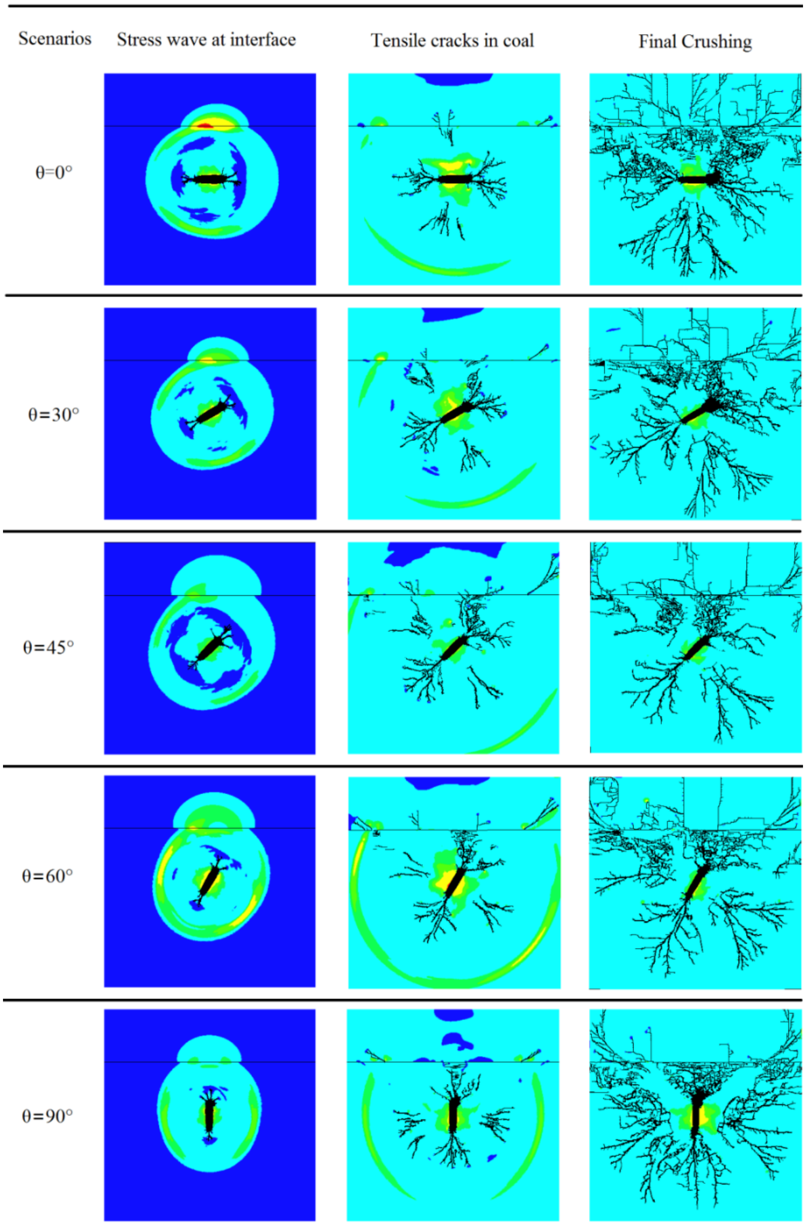

Fig. 7 The explosion stress contours of different states at different angles

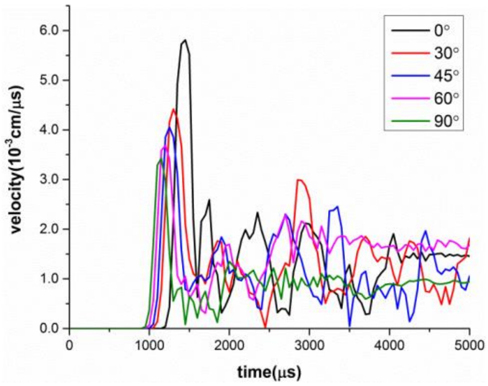

Fig. 8 Vibration velocity curves at point 1#

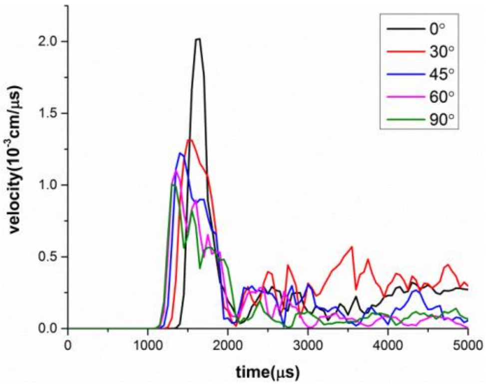

Fig. 9 Vibration velocity curves at point 2#

"mushroom shape" stress contour is formed at the interface of the coal and rock, and a stress concentration region is generated at the interface. The stress wave spreads outward in an elliptical shape, which produces a strong compression effect on the coal. Due to the high compressive strength of the coal, the unbroken coal produces elastic strain and accumulates a large amount of elastic potential energy inside. The accumulated elastic potential energy is released rapidly after the stress wave passed, causing excessive stretching to form a low stress region.

As the stress wave continues to propagate outward, the coal inside the range of the stress wave is subjected to tensile stress. Due to the low tensile strength of the coal, the tensile cracks generate under tensile stress and propagate outward after the stress wave passed. The blast cracks are densely at both ends of the charge, showing a "root-like" through the borehole. Divergent cracks are generated at a certain distance on both sides of the charge. The cracks present "petal" damage around the borehole. At the same time, the rock also exhibits tensile cracks under the action of stress wave, and spreads from the interface to the interior of the rock. The cracks formed in the rock are significantly less than those in the coal. This is due to the attenuation of the stress wave propagating into the rock, and the tensile strength of the rock is greater than that of the coal. After 4ms of explosion, the crushing process of the rock was basically completed. A large number of "petal" cracks formed in the coal around the borehole, and a small number of vertical cracks appear in the interior of the rock near the interface.

As the angle increases between the borehole and the coal-rock interface, the "butterfly" damage rotates counterclockwise. When the explosion crack propagates from the coal to the rock, the phenomenon of "suspending" occurs at the interface of the coal and rock, and the number of cracks in the rock tends to decrease gradually. Under the blocking influence of the interface, the number of cracks in the coal first decreases and then increases, then decreases and increases. The number of cracks in the rock gradually decreases and spreads to both sides. When the borehole is horizontally arranged, that is, when the angle between the borehole and the coal-rock interface is 0°, more cracks are generated in the coal, and the number of cracks in the rock is maximized, and the overall crushing effect is the best. It can be seen from the final crushing effect diagram that in order to make the best overall crushing effect of the coal and rock, the angle between the borehole and the interface should be minimized. When the angle between the borehole and the coal and rock interface is 45° and 90°, the number of cracks is slightly larger than that of the angle at 30° and 60°. The specific conditions need to be quantitatively analyzed by the following methods.

The fracture of coal and rock can be expressed indirectly by the vibration velocity of the particles. The vibration velocity of the two points 1# and 2# measured at different angles are shown in Fig. 8 and Fig. 9 below.

From the measuring point 1#, the vibration velocity of the explosion stress wave at the interface of the coal and rock is known. From the measuring point 2#, it can be seen that the explosion stress wave causes the particle vibration in the rock when entering the rock from the coal. It can be seen from Fig. 8 that a large peak appears first in the vibration velocity curve of the coal at the measuring point 1#, and then the tail disturbance is large. Fig. 9 shows that the vibration velocity curve of the rock mass at the measuring point 2# also first appears a large peak, but the tail disturbance is smaller, which is mainly due to the large hardness index of the rock. From the vibration velocity curves shown in Fig. 8 and Fig. 9, it can be seen that when the angle between the borehole and the coal and rock interface is 0°, the vibration velocity at measuring point 1#, 2# is significantly larger than that of other angles. It indicates that the overall fracture of the coal and rock is seriously at this time, which is consistent with the final fracture effect diagram obtained by the simulation.

For the numerical calculations carried out in this paper, the degree of fracture of coal and rock can also be expressed by the ratio of the number of failure units to the total number of units. The number of failure units and the number of coal units and explosive units in the numerical calculation results are got, and the peaks of the particle vibration velocity in Fig. 8 and Fig. 9 are got as shown below in Table 4.

Table 4 shows the number of specific meshes obtained by meshing coal and explosive materials by means of sweep meshing. The number of failure units is the number of units that are automatically deleted when the material is under overstressed. The fracture degree of coal and rock should be determined by the ratio of the number of failure units to the total number of coal and rock and explosives units.

Table 4 The coal crushing degree and peak velocity of measuring points

Angle	Explosive units	Coal units	Rock units	Failure units	Fracture degree/%	Peak velocity at 1# 10^{-3}cm/μs	Peak velocity at 2# 10^{-3}cm/μs
0°	120	88666	40000	14140	10.98	5.81	2.02
30°	120	88699	40000	11687	9.07	4.42	1.31
45°	120	89142	40000	11948	9.24	4.05	1.22
60°	120	89807	40000	11131	8.57	3.69	1.10
90°	120	88942	40000	12151	9.41	3.43	1.00

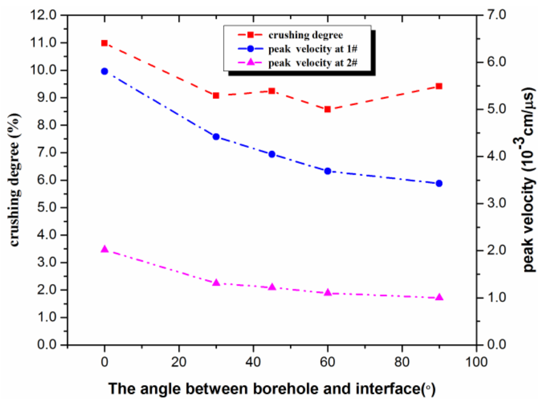

Fig. 10 The relationship between the angle and crushing degree and the peak velocity

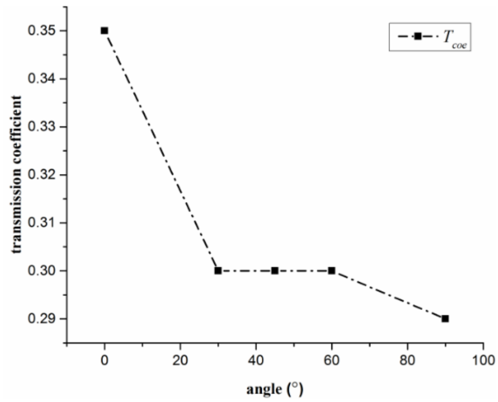

Fig. 11 The relationship between the angles and the transmission coefficient

For the relationship between the fracture degree of the coal and rock in the Table 4 and the peak value of the vibration velocity at the points 1# and 2#, the curve is shown in Fig. 10 below.

It can be seen from Fig. 10 that as the angle between the borehole and the coal-rock interface increases, the peak velocity of the particle at the measuring point 2# decreases gradually and tends to be stable, which decreasing from about 2.0×10-3 cm/μs to about 1.0×10-3 cm/μs. That is, the energy of the explosion stress wave from the coal into the rock is gradually reduced, and the crushing effect on the rock is gradually weakened, and finally it is hardly affected by the angle. The peak value of the vibration velocity at the point 1# is also gradually decreasing with the increase of the angle between the borehole and the coal-rock interface. It is reduced from about 5.7×10-3 cm/μs at an angle of 0° to about 3.4×10-3 cm/μs at 90°, and the downward trend is slowed down gradually.

The fracture of coal and rock should be the sum of coal cracks and rock cracks, which is characterized by the "*W*" trend of decreasing first, then increasing and then decreasing and increasing, which is consistent with the simulated fracture diagram. When the angle between the borehole and the interface is 0°, the fracture degree of the coal and rock (about 11%) is significantly larger than 9.4% when the angle is 90°. When the angle between the borehole and the coal and rock interface is 45°, the fracture degree of the coal rock shows a small peak, about 9.2%. The degree of fragmentation is less than 9.4% at an angle of 90°. Therefore, in the process of pre-blasting of top coal caving, in the case of technical permission, the angle between the borehole and the coal-rock interface should be minimized, which can improve the overall crushing effect of the coal and rock and get a good economic benefits.

5.2 Transmission coefficient

The phenomenon of "suspending" at the interface of coal and rock indicates that the explosion stress wave is obviously attenuated when enters from the coal to the rock. The transmission coefficient of the blast stress wave from the coal into the rock mass can be expressed by the ratio of the peak of vibration velocity from the two sides at the interface (Zhao *et al*. 2017, Zhao and Cai 2001).

$$T_{coe} = \frac{V_{tra}}{V_{inc}} \tag{17}$$

In the equation, V_{tra} is the peak value of the vibration velocity after the stress wave enters into the rock, m/s; V_{inc} is the peak value of the vibration velocity after the stress wave enters into the rock, m/s.

According to the Eq. (2), the ratio of the peak velocity of the points 1# and 2# in Table 4 is calculated, and the relationship between the transmission coefficient and the angle is shown in Fig. 11.

It can be seen from Fig. 11 that as the angle between the borehole and the coal-rock interface increases, the transmission coefficient of the explosion stress wave gradually decreases from the coal into the rock. The transmission coefficient was rapidly reduced from 0.35 at the angle of 0° to 0.30 at the angle of 30°. The transmission coefficient then remained steady then decreased to 0.29 at the angle of 90°. This indicates that the larger the angle between the borehole and the coal-rock interface, the greater the loss of energy generated by the explosion when entering the rock, and the smaller the crushing effect on the rock.

5.3 Different distances

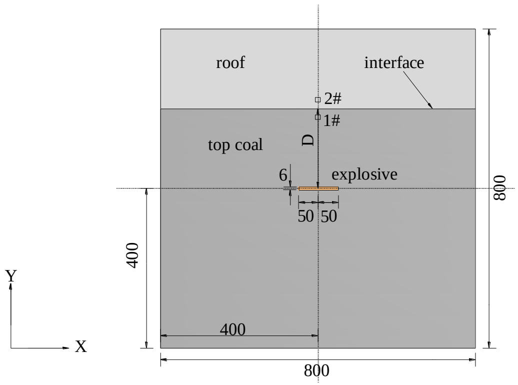

Fig. 12 Model with different distances (cm)

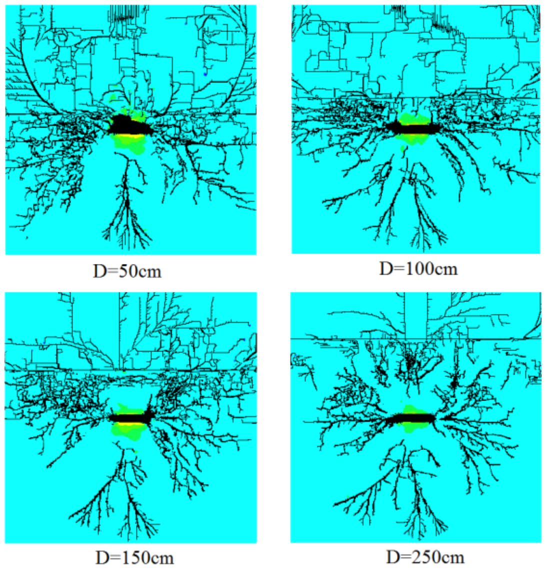

Fig. 13 Crushing effects of coal-rock at different distances

Aiming at the influence of the distance between the charge and the interface on the fracture effect of coal and rock, the model shown in Fig. 12 is designed. When the angle between the borehole and the coal-rock interface is 0°, that is, the charge and the interface are arranged in parallel, the influence of the distance between the charge and the coal-rock interface on the fracture effect of the coal-rock is studied.

As shown in Fig. 12, the distance between the charge and the coal-rock interface is D, the model size and the charge position are fixed, the coal and rock interface is moved to make D is 50 cm, 100 cm, 150 cm and 250 cm, respectively. As D is 200 cm, the charge and the interface are arranged in parallel, and the fracture of the coal and rock at the distance of 200 cm is same as the case of the previous study when the inclination angle is 0°, and is omitted here. The numerical calculation of the blasting of coal and rock under different conditions is carried out, the calculation results are post-processed, and the final crushing effect of the coal and rock is shown in Fig. 13 below.

As shown in Fig. 13, the coal-rock interface has a significant blocking effect on the propagation of stress waves. It is manifested that the number of cracks in the coal is large and dense, while in the rock is less and sparse. At

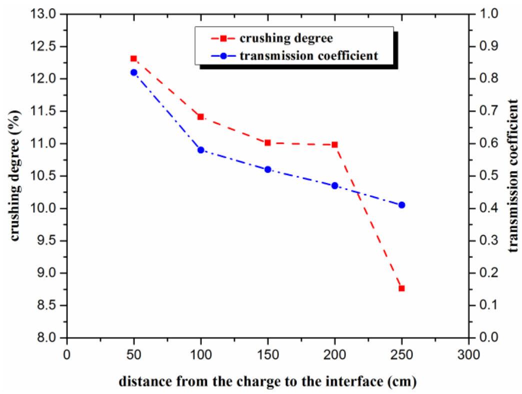

Fig. 14 Relationship between distance and crushing degree and the transmission coefficient

the interface of coal and rock, cracks are suspended. With the increase of the distance from the interface of coal and rock, the number of cracks in coal and rock is gradually reduced, and the overall degree of fragmentation is reduced. When D=50 cm, that is, the distance from the interface of the coal and rock to the charge is 50 cm, the number of cracks generated in the coal and rock is the largest. The interface of coal and rock is severely broken due to the close proximity of the charge to the interface. The borehole is damaged near the interface. This is because the borehole is close to the interface, and the blast stress wave is reflected at the interface and forming a tensile wave, which caused a tensile damage to the borehole. At a certain distance from the ends of the charge, the rock forms a pin-shaped crack extending inward from the interface of the coal and rock and converges toward the middle. At D=100 cm, the borehole and interface are less damaged, and the number of cracks in the rock is less. As the distance from the charge to the interface increases, the number of cracks in the rock gradually decreases and vertical cracks appeared, and the cracks gradually converge directly above the charge. This is because the effect of the explosive stress wave generated at both ends of the strip charge on the interface is gradually reduced as the distance from the charge to the interface increases. The cracks in the rock are mainly caused by the damage of the rock when the stress wave generated on the upper side of the strip charge is transmitted into the rock.

By using the above analysis method, the crushing degree of the coal and rock and the transmission coefficient of the stress wave from the coal into the rock are quantitatively analyzed, and the specific values obtained are shown in Fig. 14 below.

It can be seen from Fig. 14 that as the distance from the interface of the coal and rock to the charge increases, the crushing degree of the coal and rock and the transmission coefficient of the stress wave gradually decrease. The crushing degree of the coal and rock is about 12.3% at the distance of 50 cm from the charge to the interface, and decreases slowly to about 11% at the distance of 200 cm. When the distance between the charge and the interface is 250 cm, the crushing degree of the coal and rock is rapidly reduced to about 8.2%. This may be due to the fact that the stress wave is weaken when reflected from the interface as the charge and the interface exceed a certain distance, which is not enough to cause more tensile cracks in the coal and leads to a rapid decrease in the crushing degree of the coal and rock. The stress wave transmission coefficient was rapidly reduced from about 0.83 at the distance of 50 cm to about 0.55 at the distance of 100 cm, and then slowly decreased to about 0.4 at the distance of 250 cm. This is mainly because the distance from the charge to the interface is 50cm and the stress wave generated by the explosion of the explosive is strong enough, causing serious damage to the interface and more stress waves to enter into the rock and increasing the transmission coefficient of the stress wave.

As the calculated results shown in title 3.3, the crushing radius is 14.6 cm and the fracturing radius is 35.8 cm, which is 50.4 cm in total. Therefore, when the distance from the borehole to the interface is set up as 50 cm, the original damage zone should reach at the interface. And then the stress wave was reflected from the interface to the coal and expanded the fractures to propagate further.

6. Conclusions

By changing the angle between the borehole and the coal-rock interface, the numerical simulation of the top coal blasting was carried out. The simulation results were post-processed and the following conclusions were drawn.

(1) When the explosive stress wave enters the rock from the coal, the propagation velocity is accelerated, and a "mushroom-like" explosion stress contour is formed at the interface of the coal and rock. The crushing of the coal is mainly due to the accumulation of a large amount of elastic potential energy in the coal when the explosion stress wave compresses the coal. And then when the stress wave passes, the elastic potential energy in the coal is quickly released and the tensile fracture is formed by excessive stretching. The explosion crack of the coal at the two ends of the columnar charge is connected to the borehole by "tree root". Cracks are generated at a certain distance on both sides of the charge, and the whole crack is formed as "petal" around the borehole.

(2) The explosion crack is blocked by the interface of coal and rock, and there is a phenomenon of "suspending". By comparing the final blasting effect and the ratio of the number of failure units to the total number of units, it can be seen that with the increase of the angle between the borehole and the coal-rock interface, the crushing degree of the coal and rock first decreases, then increases, then decreases and then increases as characterized by the "*W*" trend. When the angle between the borehole and the interface of the coal and rock is 0°, the overall degree of fracture is the largest, about 11%.

(3) The vibration velocity curves of the two measuring points in the coal and rock at the interface indicate that the peak velocity in the rock and the coal gradually decreases with the increase of the angle between the borehole and the interface. The transmission coefficient of the explosion stress wave from the coal to the rock increases with the increase of the angle between the borehole and the interface. The transmission coefficient is the largest when the angle is 0°, which is 0.35.

(4) When the charge is arranged in parallel with the coal-rock interface, as the distance between the charge and the coal-rock interface increases, the degree of fracture of the coal and rock decreases slowly and then decreases rapidly. The stress wave transmission coefficient decreases rapidly first and then slowly decrease. When the distance between the charge and the interface is 50 cm, the stress wave transmission coefficient and the crushing degree of the coal and rock are the largest, which is 0.83 and 12.3%, respectively.

Acknowledgments

The authors thank Mr. Jhon Silva-castro for providing suggestions and the supports from Natural Science Foundation of China (No.51827901).

Conflict of Interest

The authors declare that they have no conflict of interest.

References

Ah, X. (1980), *Physical Process of Rock Blasting in Minin*, Metallurgical Industry Press Beijing.

Bai, J.Z. (2005), *Theoretical Basis and Case Analysis of LS-DYNA3D*, Science Press, Beijing.

Biao, L. and Guoliang, B. (2019), "Finite element modeling of bond-slip performance of section steel reinforced concrete", *Comput. Concrete*, **24**(3), 237-247. https://doi.org/10.12989/cac.2019.24.3.237.

Byers, B.W. (2002), "Critical review of theories of steady non-ideal two-dimensional detonation of condensed explosives, Confidential Report to HSBM participants, Mass Action, UK.

Chun-rui, L., Li-jun, K., Qing-xing, Q., De-bing, M., Quan-ming, L. and Gang, X. (2009), "The numerical analysis of borehole blasting and application in coal mine roof-weaken", *Procedia Earth Planet. Sci.*, **1**, 451-459. https://doi.org/10.1016/j.proeps.2009.09.072.

Cooper, P.W. (1996), *Explosives Engineering*, VCH Publishers Inc., New York, USA.

Dai, J. (2002), *Rock Dynamics and Blasting Theory*, Metallurgical Industry Press, Beijing.

Esen, S. (2008), "A non-Ideal detonation model for evaluating the performance of explosives in rock blasting", *Rock Mech. Rock Eng*., **41**(3), 467-497. https://doi.org/10.1007/s00603-006-0119-2.

Hao, Y.X. (2016), "Study on rockburst of wudong near-vertical coal seams and impact protection with constant resistance and large deformation supporting", China University of Mining and Technology, Beijing.

Kury, J.W., Hornig, H.C., Lee, E.L., McDonnel, J.L., Ornellas, D.L., Finger, M., ... & Wilkins, M.L. (1965), "Metal acceleration by chemical explosives", *Proceedings of the Fourth Symposium (International) on Detonation*, US Government Printing Office Washington, DC, October.

Lee, E.L., Hornig, H.C. and Kury, J.W. (1968), "Adiabatic expansion of high explosive detonation products", Report

UCRL-50422, University of California, Lawrence Radiation Laboratory, Livermore, CA, USA.

Li, S., Fan, C., Luo, M., Yang, Z., Lan, T. and Zhang, H. (2017), "Structure and deformation measurements of shallow overburden during top coal caving longwall mining", *Int. J. Min. Sci. Tech.*, **6**(27), 1081-1085. https://doi.org/10.1016/j.ijmst.2017.06.005.

Li, Z.L., He, X.Q., Dou, L.M., Song, D.Z. and Wang, G.F. (2018), "Numerical investigation of load shedding and rockburst reduction effects of top-coal caving mining in thick coal seams", *Int. J. Rock Mech. Min. Sci.*, **110**, 266-278. https://doi.org/10.1016/j.ijrmms.2018.08.005.

Liu, F., Silva, J., Yang, S., Lv, H. and Zhang, J. (2019), "Influence of explosives distribution on coal fragmentation in top-coal caving mining", *Geomech. Eng.*, **18**(2), 111-119. https://doi.org/10.12989/gae.2019.18.2.111.

Livermore Software Technology Corporation (LSTC) (2003), LS-DYNA Keyword User's Manual, Version 970, Livermore, CA.

Lu, C.P., Dou, L.M., Liu, B., Xie, Y.S. and Liu, H.S. (2012), "Microseismic low-frequency precursor effect of bursting failure of coal and rock", *J. Appl. Geophys.*, **79**, 55-63. https://doi.org/10.1016/j.jappgeo.2011.12.013.

Mahdi, A., Roozbeh, T. and Aliakbar, Y. (2019), "Simulation of cyclic response of precast concrete beam-column joints", *Comput. Concrete*, **24**(3), 223-236. https://doi.org/10.12989/cac.2019.24.3.223.

Naseri, R. and Behfarnia, K. (2019), "A numerical study on the seismic behavior of a composite shear wall", *Comput. Concrete*, **22**(3), 279-289. https://doi.org/10.12989/cac.2018.22.3.279.

Nicieza, C.G., Díaz, M.R., Fernández, M.Á. and Vigil, A.Á. (2012), "Characterization of ground from the point of view of its excavatability", *Eng. Geol.*, **12**(6), 8-18. https://doi.org/10.1016/j.enggeo.2011.11.004.

Pradhan, S.P., Vishal, V. and Singh, T.N. (2018), "Finite element modelling of landslide prone slopes around Rudraprayag and Agastyamuni in Uttarakhand Himalayan terrain", *Nat. Hazard.*, **94**(1), 181-200. https://doi.org/10.1007/s11069-018-3381-1.

Prem, P.R., Thirumalaiselvi, A. and Verma, M. (2019). "Applied linear and nonlinear statistical models for evaluating strength of Geopolymer concrete", *Comput. Concrete*, **24**(1), 7-17. https://doi.org/10.12989/cac.2019.24.1.007.

Saiang, D. (2009), "Stability analysis of the blast-induced damage zone by continuum and coupled continuum-discontinuum methods", *Eng. Geol.*, **116**, 1-11. https://doi.org/10.1016/j.enggeo.2009.07.011.

Sanchidrián, J.A., Castedo, R., López, L.M., Segarra, P. and Santos, A.P. (2015), "Determination of the JWL constants for ANFO and emulsion explosives from cylinder test data", *Central Eur. J. Energ. Mater.*, **12**(2), 177-194.

Shang, X.J., Su, J.Y. *et al.* (2005), *Dynamic Analysis Method and Engineering Example of ANSYS/LS-DYNA3D*, China Water Conservancy and Hydropower Press, Beijing.

Shi, D.Y., Li, Y.C. and Zhang, S.M. (2005), *Display Dynamic Analysis Based on ANSYS/LS-DYNA8.1*, Tsinghua University Press, Beijing.

Suo, Y.L. (2004), "Basic study on technology of pre-blast weakening hard top coal in fully mechanized caving faces", Xi'an University of Science and Technology, Xi'an.

Wang, F., Tu, S., Yuan, Y., Feng, Y., Chen, F. and Tu, H. (2013), "Deep-hole pre-split blasting mechanism and its application for controlled roof caving in shallow depth seams", *Int. J. Rock Mech. Min. Sci.*, **64**, 112-121. https://doi.org/10.1016/j.ijrmms.2013.08.026.

Wang, J. and Li, Y. (2017), "Thick seam coal mining and its ground control", *Adv. Coal Mine Ground Control*, 379-407. https://doi.org/10.1016/B978-0-08-101225-3.00008-6.

Wang, J.C., Chen, Z.H., Bai, X.J. *et al.* (2000), "Study on parameters of pre-blasting of top coal in fully mechanized mining of hard thick seam", *Coal*, **3**, 1-4.

Xu, T. (2019), "Blasting vibration safety criterion of surrounding rock of a circular tunnel", *Geotech Geol Eng.*, **37**(4), 3077-3084. https://doi.org/10.1007/s10706-019-00826-z.

Yan, P., Zhao, Z., Lu, W., Fan, Y., Chen, X. and Shan, Z. (2015), "Mitigation of rock burst events by blasting techniques during deep-tunnel excavation", *Eng. Geol.*, **18**(8), 126-136. https://doi.org/10.1016/j.enggeo.2015.01.011.

Yang, J.X. (2015), "Study on confined blasting control mechanism of hard coal rock with high safety and efficiency and test analysis", China University of Mining and Technology, Xuzhou.

Yang, S.Y. (1993), *Dynamics Foundation of Rock Blasting*, Coal Industry Press, Beijing.

Yasitli, N.E. and Unver, B. (2005), "3D numerical modeling of longwall mining with top coal caving", *Int. J. Rock Mech. Min. Sci.*, **42**(2), 219-235.

Zhang, Q. (1998), *Analysis and Application of Dynamics Blasting Engineering*, Coal Industry Press, Beijing.

Zhao, J. and Cai, J.G. (2001), "Transmission of elastic P-waves across single fractures with a nonlinear normal deformational behavior", *Rock Mech. Rock Eng.*, **34**, 5-15.

Zhao, J.J., Zhang, Y. and Ranjith, P.G. (2017), "Numerical simulation of blasting-induced fracture expansion in coal masses", *Int. J. Rock Mech. Min. Sci.*, **100**, 28-39.

CC